A high sensitive impedimetric label free immunosensor for Ochratoxin measurement in cocoa beans

Francesca Malvano[a], Donatella Albanese*[a], Roberto Pilloton[b], Marisa Di Matteo[a]

[a]Department of Industrial Engineering, University of Salerno, Via Giovanni Paolo II 132, 84084, Fisciano (SA), Italy.
[b]Institute of Atmospheric Pollution Research of the National Council of Research (CNR), Via Salaria , Montelibretti, Roma,Italy

***Corresponding author : dalbanese@unisa.it; Phone +3989964129**

Abstract

In this work the development and optimization of an impedimetric label free immunosensor for the detection of Ochratoxin A (OTA) is reported.

Two antibody immobilization methods (oriented and not oriented) were compared highlighting a lower limit of detection (5 pg/ml) for the not oriented immobilization but a closer linear range in contrast to oriented anti – OTA immunosensors which showed linearity in the range of 0.01- 5 ng/mL OTA. The analysis of the Atomic Force Microscopy (AFM) images showed two different nanostructures indicating that the use of oriented immobilization created a more ordered and highly dense antibody surface. Finally the oriented immunosensor was used to quantify OTA in spiked cocoa bean samples and the results were compared with those registered with competitive ELISA kit. The immunosensor was sensitive to OTA lower than 2 μg/kg that represents the lower acceptable limit of OTA established by European legislation for the common food products.

Keywords: Immunosensor, Ochratoxin A, Electrochemical Impedance Spectroscopy, Atomic Force Microscopy

1. Introduction

Mycotoxins are toxic secondary metabolites responsible for the contamination of approximately 25% of the world's crops, causing spoilage of agricultural products. In pollutants risk assessment, experts consider these contaminants as the most important chronic dietary risk factor (Prieto-Simon, Campas, Marty & Noguer, 2008).

Ochratoxin A (OTA) is a secondary metabolite produced by several species of *Aspergillus* and *Penicillium* fungi. The toxin, which is a nephrotoxic and nephrocarcinogenic compound, has mainly been found in cereals but significant levels of contamination may also occur in coffee, cocoa beans, wine, dried fruits, beer and grape juice spices. OTA is a proven carcinogen in animals and is classified as a class 2B, possible human carcinogen by the International Agency for Research on Cancer (Reddy & Bhoola, 2010). The National Toxicology Program (NTP) has designated OTA as "reasonably anticipated to be a human carcinogen" based on sufficient evidence of carcinogenicity in experimental animals (Clark & Snedeker, 2006). Regulations relating to mycotoxins have been established in many countries to protect the consumer from the harmful effects of these compounds. In several countries, these contaminants are subject to legislation that is based on the establishment of an Acceptable Daily Intake (ADI) or Tolerable daily intake (TDI). In the European Union the acceptable limits established for OTA in various foodstuffs are listed in Commission Regulation (EC) No 1881/2006 and ranged from 10 μg/kg for instant coffee and dried vine fruits to 0.5 μg/kg for dietary foods intended specifically for infants. OTA is a heat-stable molecule within the range of

conventional food processing temperatures and no destruction occurs under normal cooking conditions such as boiling and frying, or even following pasteurization. Thus the accurate knowledge of OTA contamination level in food products represents a key factor in the food safety at worldwide level. Research studies have been conducted to develop appropriate methods for the detection of OTA in food and feed samples (Kaushik, Arya, Vasudev & Bhansali 2013). Traditional methods include gas chromatography, thin layer chromatography, capillary electrophoresis and high-performance liquid chromatography. However, these techniques require expensive equipment as well as complicated and time-consuming solvent cleanup steps. Owing to their high sensitivity, good specificity, and less dependence on sample cleanup, electrochemical sensors based on immunological procedures seem most promising, thanks to their low cost, compatibility with miniaturization and portability (Muchindu et al., 2010). Therefore, immunosensors have aroused a very great interest with expectations of providing fast and highly sensitive detection of proteins, peptides, toxins, viruses and bacteria or part of these, finding widespread applications in clinical diagnostics, food safety and environmental monitoring.

In the field of food safety some studies have been focused on the development of electrochemical immunosensor for OTA determination; Prieto-Simon et al. (2008), Bonel, Vidal, Duato & Castillo, (2010) and Liu, Yang, Zhang & Yub (2013) studied indirect competitive enzyme-linked immunosorbent assays (ELISA) strategies, developing labelled immonusensors for wine, wheat and corn samples analysis respectively. All measurements were conducted by differential pulse voltammetry technique. In these cases, the immunosensors required a label attached to the target: during readout the amount of label is detected and assumed to correspond to the number of bound targets. However, labelling a biomolecule can drastically change its binding properties, and the yield of the target-label coupling reaction is highly variable (Daniels & Pourmanda, 2007). Moreover, the use of labels is also a source of higher costs and analysis times (Ricci, Volpe, Micheli & Palleschi, 2007).

For these reasons, in the last years, the potential use of Electrochemical Impedance Spectroscopy (EIS) technique has been examined in the immunosensor development; it is, in fact, a powerful, nondestructive and informative technique, which can be used to study the electrical properties of the sensing device interface and to trace the reactions (Ciania et al., 2012). The application of EIS on modified electrodes on which antibodies have been immobilized let to develop label free immunosensors based on the impedimetric change that occurs when the immunocomplex occurred on the electrodes surface. Muchindu et al., (2010) and Radi, Munoz-Berbel, Latesc & Martyc (2009) reported the development of impedimetric immunosensors for the detection of OTA in a linear range of 2-10 and 1–20 ng/mL respectively. Studies on the development of electrochemical aptasensor for detection of OTA have been recently published (Mishra, Hayat, Catanante, Istamboulie & Marty, 2015). Even if aptamers offer many advantages in contrast to antibodies, i.e they are easier and more economical to produce, the analysis of food samples require clean up procedures increasing time and cost analysis and thus reducing the advantages of the biosensors.

An important aspect that has to be considered during the fabrication of an immunosensor is the orientation of the sensing molecules on solid phase for improving sensitivity, specificity, and analyte-binding capacity.

From the above the aim of this work is the development of a highly sensitive label-free impedimetric immunosensor for the detection of OTA in food samples. A Self Assembled Monolayer (SAM) procedure coupled with the oriented immobilization of the monoclonal anti-OTA was used for the construction of the immunosensor and the EIS with Cyclic Voltammetry were used to characterize the immobilization steps and the performance of the immunosensors. The sensitivity and the topography by Atomic Force Microscopy (AFM) of oriented and not oriented immunosensors was also investigated. Finally the immunosensor was used to quantify OTA in spiked cocoa bean samples and the results compared with competitive ELISA kit.

2. Materials and Methods

2.1 Reagents

4-mercaptobenzoic acid (MBA, 99%), 2-(*N*-morpholino)ethanesulfonic acid (MES >99.5% purity), N-Hydroxysucciminide (NHS, 99%), N-(3-Dimethylaminopropyl)-N′-ethylcarbodiimide hydrochloride (EDC, >99%), Sulfuric acid (H_2SO_4, 99.9%), Ethanolamine ($NH_2CH_2CH_2OH$, >99.5%), Potassium hexacyanoferrate (III) ($[Fe(CN)_6]^{3-}$, >99%), Tween 20, Ethanol (>99.8%) and Ochratoxin A were purchased from Sigma-Aldrich (Milano, Italy). Potassium ferrocyanide ($[Fe(CN)_6]^{4-}$) was obtained from Carlo Erba reagent (Milano, Italy). Anti-Ochratoxin A antibody (anti-OTA)(1 mg/mL) was purchased from Abcam (Cambridge, United Kingdom), while Protein A/G (5 mg/mL, 59.7 kDa, >98%) was obtained from BioVision Inc. (San Francisco, USA). NaH_2PO_4, Na_2HPO_4, NaCl and KCl used in the preparation of phosphate buffered saline (PBS: 0.1 M KCl, pH 7.4) were received from Sigma Aldrich (Milano, Italy) .

2.2 Apparatus

The electrochemical measurements were carried out with a computer-controlled Autolab PGSTAT 204 Potentiostat and Nova software. Au thin-film single-electrodes were obtained from Micrux Technologies (Oviedo, Spain). The electrodes incorporate a conventional three – electrode configuration, with an Au working (diameter 1 mm), reference and counter electrodes.

2.3 Immunosensor Manufacturing

Before modification, gold electrodes were cleaned by applying 13 potential cycles between -1.0 and +1.3 V with 100 mV/s scan rate in 0.05 M sulfuric acid. SAM was carried out on the surface of the electrode using an ethanol solution containing MBA 30 mM under a constant potential of 1.2 V for 20 min.

The terminal carboxylic groups on gold electrode surface were activated by dropping on the Au

modified electrode a solution of 75 mM EDC and 15 mM NHS in 100 mM MES buffer (pH 7.4) for 2 hours.

Thereafter, the immobilization of anti-OTA was carried out in oriented and not oriented way. In the oriented immobilization method 20 μL of Protein A/G 5 mg/mL were dropped on the modified electrode and left to react for 1hour. After incubation, 100 μL of 1 M ethanolamine (pH 8.5) solution was dropped onto the modified surface and incubated for 15min to block unreacted active sites. After thorough rinsing with PBS buffer, the modified electrode was covered with 10 μL of anti-OTA solution at four different concentrations (0.5 ng/mL, 1 ng/mL, 5 ng/mL, 10 ng/mL) for 30 min at room temperature. Finally the electrode was rinsed in PBS to remove unbound antibodies. In the not oriented construction of the immunosensor, the anti-OTA solution was added after the activation of carboxylic groups with EDC/NHS. Then the electrode was rinsed in PBS to remove unbound antibodies and finally the unreacted active sites were blocked with 1 M ethanolamine.

The schematic diagram of the immunosensors fabrication is presented in Fig.1.

2.4 Experimental Measurement

EIS measures the response of an electrochemical system to an applied oscillating potential as a function of the frequency resulting in an impedance spectra (Nyquist plot) where the complex impedance is displayed as the sum of the real and imaginary components (Z^I and Z^{II} respectively).

For electrochemical impedance studies, a sinusoidal AC potential (10 mV) in the frequency range from 0.1 to 10^5 Hz was super imposed to a 0.00 mV (vs. reference electrode) DC potential. The measurements were performed in a solution of 1 mM ferri/ferrocyanide redox couple ($[Fe(CN)_6]^{4-/3-}$, 1:1) in PB, pH 6.8, as background electrolyte at room temperature.

The CV was also used to characterize each step of electrode modification and anti-OTA immobilization. The measurements were performed from -0.6 to 0.6 V vs. reference electrode with a scan rate of 0.05 V/s; the redox couple used for the CV was the same as that used for impedance measurements, 1 mM ferri/ferrocyanide redox couple ($[Fe(CN)_6]^{4-/3-}$,1:1) in PB, pH 6.8.

For the OTA measurement, 10 μL of OTA at different concentrations in PBS were dropped onto the working area of the immunosensor and incubated for 20 min. Before the impedance measurements the immunosensor was rinsed thoroughly with copious amount of bi-distilled water.

2.5 AFM studies

AFM studies were performed by using Veeco Dimension 3100 AFM with Nanoscope III controller. Measurements were carried out by using a silicon cantilever with a nominal tip radius of 20 nm. Topographic images were taken in tapping mode with a scan size of 1x1 μm.

2.6 Preparation of cocoa beans samples

The preparation of the cocoa bean samples was according to the procedure described in I'screen Ochra Elisa kit (Tecna, Italy). 2.5 g of finely grinded cocoa beans was added to 5 mL of 0.1 M phosphoric acid and 50 mL of chloroform; the solution was shaken in a low – speed shaker (400 rpm) for 15 min. 25 mL of filtrate were collected and added to 5 mL of the 0.13 M sodium bicarbonate solution; the solution was shacked for 30 seconds. The upper aqueous phase was recovered and centrifuged to remove solvent traces. Finally 4mL of sodium bicarbonate solution was added to 1 mL of surfactant.

This procedure was applied for four different amounts of OTA spiked to grinded cocoa bean samples in order to obtain 1, 1.5, 2.5 and 5μg/kg. The total samples analyzed were 12, three for each OTA concentration. The results obtained by the immunosensors were compared with those measured with the competitive Elisa kit (I'screen Ochra Elisa kit -Tecna, Italy) for OTA detection.

3. Results and discussion

3.1 Assembling of immunosensor

The design of the immobilization layout is a very important factor in the performance of immunosensors, as it greatly affects both the sensitivity and the specificity of the biointerface.

187 The surface modification of the Au electrodes for the preparation of OTA oriented immunosensor
188 was monitored using EIS and CV.
189 The voltammogramms of the Au electrode at the different immobilization steps display well defined
190 anodic and cathodic peaks due to the reversible interconversion of $Fe(CN)_6^{3-/4-}$ (Fig. 2A). The
191 formation of the consecutive layers, as described in Fig. 1, causes the decrease of both peaks due to
192 hindering effects of the layers on the electron transfer rate.
193 The Nyquist plots belonging to the all fabrication steps of the immunosensor were shown in Fig. 2B.
194 The linear part at lower frequencies corresponds to a diffusion process while the semicircle diameter
195 at higher frequencies corresponds to an electron transfer resistance. Because this last property
196 depends on the dielectric and insulating features at the electrode/electrolyte interface, it can be used
197 to describe the interface properties of the electrode (Prabhakar, Matharu & Malhotra, 2010).
198 As expected, when chemical species get covalently immobilized on the Au electrode surface, the
199 impedance of the electrochemical system increases (Fig. 2B). This could be ascribed to the blocking
200 layer coating on electrode surface, which became thicker with the assembly procedure.
201 In particular, as result of the immobilization on the electrode surface of MBA, protein A/G and the
202 final addition of ethanolamine, the diffusion of the redox probe close to the Au modified surface was
203 dramatically reduced. The permeability of $Fe(CN)_6]^{4-/3-}$ through the immobilization layers was
204 strongly reduced with a significant increase of the electron transfer resistance. A further increase of
205 the impedance was observed when the anti-OTA is immobilized.
206 The impedance and cyclic voltammetry results revealed that the chemical and biomolecular layers
207 acted as effective barriers to the charge transfers (Anandan, Gangadharan, & Zhang, 2009; Radi et
208 al., 2009).
209
210 *3.2 Optimization of anti - OTA concentration*
211 Because the sensitivity of immunosensors depends on the immunochemical reactions of antigen with
212 the antibody, the optimization of the amount of anti – OTA on electrode surface is a discriminant

213 factor for the performances of the immunosensor in the same way as dilution of antibodies plays an
214 important role in preparation of ELISA plates.
215 For this purpose, immunosensors were produced immobilizing four different amounts (0.5 μg/mL, 1
216 μg/mL, 5 μg/mL and 10 μg/mL) of anti-OTA on the modified electrodes. Fig. 3 shows the Nyquist
217 plots of oriented OTA immunosensors at different concentrations of anti-OTA (0.5 μg/mL (Fig. 3A),
218 1 μg/mL (Fig. 3B), 5 μg/mL (Fig. 3C) and 10 μg/mL (Fig. 3D) for OTA increasing amount. The
219 Nyquist plots were fitted using Nova software by the equivalent circuit shown in the inset of Fig. 3.
220 This equivalent circuit model, commonly applied for the impedimetric immunosensor
221 characterization (Daniels et al., 2007), consists of resistive and capacitive elements, as well as a
222 Warburg element. R_s represents the resistance of the working solution while CPE (constant phase
223 element) is connected with the capacitance of the complex bioactive layer; R_{ct} is related to the electron
224 transfer resistance through the electrode surface and the Warburg impedance describes the normal
225 diffusion to the electron surface through the complex layer. In the given frequency range, the most
226 significant changes were observed in the R_{ct} values (Table S1); in particular, it can be seen the R_{ct}
227 value decreases by increasing OTA concentration for all the four different tested immunosensors.
228 These results were in agreement with Muchindu et al. (2010) who developed an OTA immunosensor
229 on Pt disk electrode modified with doped Polyaniline film. The decreasing of R_{ct} could be due to the
230 formation of immunocomplex that causes differences in the dielectric or conductivity properties of
231 the electrode surface (Darain, Park & Shim, 2004).
232 As regards the differences among the impedance spectra (Fig. 3) for the four immunosensors
233 developed, it is possible to see that the immunosensor with 1 μg/mL anti – OTA showed remarkable
234 decreases of the semicircle diameter and in R_{ct} (Table S1) for all the OTA amounts. For the
235 immunosensor at 0.50 μg/mL anti – OTA, OTA concentrations lower than 0.05 ng/mL did not bind
236 sufficiently and thus the electron transfer resistance did not show the expected decrease.

237 Finally, the immunosensor with 5 μg/mL and 10 μg/mL anti – OTA concentrations, because of high
238 density of anti-OTA, showed higher impedances even if an evident decrease of R_{ct} was observed only
239 when OTA was dropped at concentrations higher than 0.1 ng/mL. In this case the electrode surfaces
240 is so dense that the binds between anti-OTA and OTA are insufficient to cause any charge transfer
241 resistance decrease. Consequently the denser bioactive layer probably resulted in an activity loss in
242 the immunosensor performance. Hence 1 μg/mL anti – OTA was chosen as the optimal concentration
243 for the further characterization of the immunosensor.
244
245 *3.3 Analytical characteristics of Immunosensor.*
246 As discussed above the value of the equivalent circuit that showed the most remarkable differences
247 at different OTA amount was the electron transfer resistance (R_{ct}). This parameter was then used to
248 characterize the immunosensors fabricated with 1 μg/ml anti-OTA. The calibration curve was
249 obtained by plotting the logarithmic value of OTA concentrations versus ΔR_{ct}. ΔR_{ct} was calculated
250 by the following equation:
251 $$\Delta R_{ct} = R_{ct(anti\text{-}OTA)} - R_{ct\,(OTA)} \quad (1)$$
252 where $R_{ct(anti\text{-}OTA)}$ is the value of electron transfer resistance when anti-OTA is immobilized on the
253 electrode surface and $R_{ct\,(OTA)}$ is the value of electron transfer resistance after the bind between anti-
254 OTA and OTA.
255 The calibration curve showed a linear correlation in the range from 10 pg/mL to 5 ng/mL, for values
256 higher than 5 ng/mL, no linear ΔR_{ct} were observed probably due the saturation of the specific binding
257 sites (Fig. S1).
258 The limit of detection (LOD), based on the sum of average blank solution and three times the standard
259 deviation, was estimated to be 0.01 ng/mL with a response time of 30 min including the incubation
260 time. The reproducibility calculated on five different OTA immunosensors at OTA 0.3 ng/mL
261 showed a Relative Standard Deviation (RSD) of 5.6%. The possible re-use of OTA immunosensors

was also investigated. For this purpose after the immunocomplex formation between anti-OTA and OTA the electrode was dipped in 10:10:80 methanol:acetonitrile:water solution for 40 min and the immunoassay, using the same OTA concentration (0.05 ng/ml), was performed. The impedance spectra (Fig. S2) obtained after the binding anti-OTA and OTA for the immunosensor pretreated for OTA detachment showed a lower impedance highlighting a decrease of anti-OTA immobilized on the electrode surface and thus a change of the analytical performance. These results indicate the OTA immunosensor as a single use device. Finally the storage stability was also determined. For this purpose different immunosensors were stored for 21 days at 4 °C without chemical preservatives and characterized at regular interval times. After the investigated storage period the immunosensors showed a negligibile loss of activity.

3.4 Oriented and not oriented anti – OTA immobilization

The method of biomolecules immobilization on conductive surfaces plays a crucial role in the performance of an immunosensor. The method for the immobilization of antibodies used for immuno-affinity assays should orient the interacting sites (Fab) of antibodies towards the test solution with the antigen molecules. Protein A/G is an immunoglobulin (Ig)-binding protein that shows specificity for the heavy chains on the Fc region of antibodies, thus it effectively orients the immobilized antibodies with antigen-binding sites facing outward. When Protein A/G is not used in the immobilization procedure the covalent bond between the activated SAM and the NH_2 groups of anti-OTA occurs in non-specific position. In this condition the probability of interaction between OTA and anti-OTA decreases (Fig. 1B). In this regard, OTA immunosensors with 1μg/ml anti-OTA were fabricated using the two immobilization methods and their analytical performances were compared (Fig. S3). When the antibody immobilization occurred random, a lower charge transfer resistance was registered probably due to a lower number of antibodies immobilized on the surface of the electrode. The analytical characterization of the two immunosensors versus different concentration of OTA (Fig. S3B) showed a closer linear range but a lower detection limit (5 pg/mL) for the not oriented

288 immunosensor. This means that in case of not oriented antibodies a number of molecules, lower than
289 in the oriented one, is effectively exposed to antigen interaction and that the receptor based biosensors
290 decrease their LOD when the effectively immobilized receptor molecules are optimally minimized in
291 order to still obtain a signal from the transducer (Cremisini, Di Sario, Mela, Pilloton & Palleschi,
292 1995).
293 On the contrary in the oriented immunosensor a wider linear range and a higher sensitivity were
294 observed and thus a higher antigen – binding capacity (Kausaite-Minkstimiene, Ramanaviciene,
295 Kirlyte & Ramanavicius, 2010). The comparison of the analytical performance of the label free
296 immunosensors developed in this study with the other impedimetric bioaffinity sensors (immuno and
297 aptasensors) in the literature is reported in Table 1. The OTA oriented and not oriented
298 immunosensors reported in this study showed a wide lineare range and the lowest LOD when
299 compared with the other immunosensors.
300
301 *3.5 AFM results*
302 AFM is a very useful technique able to obtain information about the morphological characteristics of
303 the resulting surfaces of the immunosensors.
304 AFM 3D - images of an oriented and a not oriented immunosensor surface are reported in Fig. 4.
305 The surface of the oriented immunosensor (Fig. 4A) shows a number of homogeneous spheres – like
306 structures, which were expected from a densely packed protein monolayer. The surface of not
307 oriented immunosensor (Fig. 4B), instead, shows not well-distributed structures, with different sizes
308 and heights.
309 AFM "roughness analysis" parameters were chosen as key descriptors of surfaces morphology:
310 average roughness (R_a), which is the average deviation of the measured z-values from the mean-
311 plane, root-mean-square roughness (R_q), which effectively describes the standard deviation of an
312 entire distribution of z-values and maximum roughness (R_{max}) which indicates the difference between
313 the largest positive and negative z-values. The results of the roughness analysis (Table S2) showed

314 all roughness values lower for oriented surface, pointing out that, in the case of oriented antibody, a
315 more homogeneous surface is obtained.
316 Moreover, by using the Particle Analysis Method (Fig. 4 (A) and (B) inset), the mean size (diameter)
317 and the density of the nanostructures observed in a scanning size of 1 μm^2 were calculated.
318 The mean size of the oriented structures is found to be 57.22 nm, against the 121.64 nm of the not
319 oriented structures.
320 In AFM analysis, due to the tip broaden effect, the observed single spheres have larger size than those
321 of a real protein molecule. The real diameter of the structures (protein layer) can be calculated,
322 according to Zhengijan, Wang, Chen & Deng (2010), by the following formula:
323 $$D = 2\sqrt{2Rr + r^2} \quad (2)$$
324 where R is the tip radii, r is the real width of protein molecule and D is the apparent width of protein
325 molecule, respectively.
326 For a tip of 20 nm, the real size of protein structure in the oriented immunosensor was very close to
327 the theoretical estimation of Ig equal to 14.2 nm (Zhengijan et al., 2010). A higher real size (44 nm)
328 was calculated for not oriented immobilization probably due to the random covalent bond between
329 activated SAM and the anti-OTA. Moreover the higher density value (66 particles/μm^2) observed for
330 oriented immobilization in contrast to that calculated for not oriented one (13 particles/μm^2) confirm
331 the well known capability of ProteinA/G to create an ordered a highly dense antibody surface.
332
333 *3.6 Measurement of OTA in cocoa beans*
334 The feasibility of applying the proposed immunosensor for the detection of OTA in food matrices
335 was studied. We chose cocoa beans due to their complex composition that could interfere during the
336 analysis and their very low level (maximum 2 μg/kg) permitted by the European standard.
337 Cocoa bean samples were spiked with four different concentrations of OTA, and analyzed by the
338 developed immunosensors and competitive ELISA Kit for OTA detection. The sample preparation
339 used was the same for both the analytical methods. The results are shown in Table 2 where good

recovery percentage exhibited by the immunosensor is reported, too. Taking into consideration the LOD of the anti-OTA immunosensor and the dilution factors used for the OTA detection in food matrices that can range from 5 to 50, the impedimetric immunosensors developed in this study show a detection limit of 0.05 and 0.5 μg/kg respectively.

According to Table 2 the sensitivity of the label free impedimetric immunosensor developed in this work is enough to allow the detection of OTA levels in cocoa beans established by EU that recommends a concentration up to 2 μg/kg.

4. Conclusions

In this study, a label free impedimetric immunosensor for sensitive detection of Ochratoxin A in food matrices (in chocolate samples) was developed and the electrochemical impedance spectroscopy was used to investigate it. The comparison between the two immobilization procedures (oriented and not oriented antibody) used for the fabrication of immunosensors underlines the advantages of the oriented immobilization, which showed a more uniform and homogenous antibody layer that favors higher antigen – binding capacity, and sensitivity of the immunosensor.

The results obtained with AFM analysis were in good agreement with those obtained from impedance characterization studies, underlining that in case of oriented antibody a more ordered surface guarantees a higher number of molecules effectively exposed to antigen interaction. Finally the linear range, the very low detection limit and high sensitivity showed the potential of the proposed immunosensor as a highly capable analytical device for a fast OTA measurement in food matrices.

Acknowledgments

Authors thank prof. Roberto Pantani for the use of Atomic Force Microscopy and Ing. Vito Speranza for technical assistance in AFM experiments.

366

367

368 **References**

369

370 Anandan, V., Gangadharan, R., & Zhang, G. (2009). Role of SAM Chain Length in Enhancing the
371 Sensitivity of Nanopillar Modified Electrodes for Glucose Detection. *Sensors, 9*, 1295-1305.
372
373 Bonel, L., Vidal, J.C., Duato, P., & Castillo, J.R. (2010). Ochratoxin A nanostructured
374 electrochemical immunosensors based on polyclonal antibodies and gold nanoparticles coupled to
375 the antigen. *Analytical Methods*, *2*, 335-341.

376 Ciania, I., Schulzeb, H., Corriganb, D.K., Henihanb, G., Giraudc, G., Terryd, J.G., et al. (2012)
377 Development of immunosensors for direct detection of three wound infection biomarkers at point of
378 care using electrochemical impedance spectroscopy. *Biosensors and Bioelectronics, 31,* 413–418.

379 Clark, H.A., & Snedeker, S.M. (2006). Ochratoxin A: its cancer risk and potential for exposure.
380 *Journal of Toxicology and Environmental Health B, 9*, 265–296.
381
382 Cremisini, C., Di Sario, S., Mela, J., Pilloton, R., Palleschi, G. (1995). Evaluation of the use of free
383 and immobilised acetylcholinesterase for paraoxon detection with an amperometric choline oxidase
384 based biosensor. *Analytica Chimica Acta 311 (3),* 273-280.
385
386 Daniels, J.S., & Pourmanda N. (2007). Label-Free Impedance Biosensors: Opportunities and
387 Challenges. *Electroanalysis*, *19(12)*, 1239–1257.
388
389 Darain, F., Park, D.S., Park, J.S., & Shim, Y.B. (2004). Development of an immunosensor for the
390 detection of vitellogenin using impedance spectroscopy. *Biosensor and Bioelectronics, 19 (10),* 1245
391 – 1252.
392
393 Kausaite-Minkstimiene, A., Ramanaviciene, A., Kirlyte, J., & Ramanavicius, A. (2010). Comparative
394 Study of Random and Oriented Antibody Immobilization Techniques on the Binding Capacity of
395 Immunosensor. *Analytical Chemistry, 82,* 6401–6408.
396
397 Kaushik, A., Arya, S.K., Vasudev, A. & Bhansali, S. (2013). Recent Advances in Detection of
398 Ochratoxin - A. *Open Journal of Applied Biosensor, 2,* 1-11.

399
400 Liu, X., Yang, Z., Zhang, Y., & Yub, R. (2013). A novel electrochemical immunosensor for
401 ochratoxin A with hapten immobilization on thionine/gold nanoparticle modified glassy carbon
402 electrode. *Analytical Methods, 6*, 1481-1486.
403
404 Mishra, R.K., Hayat, A., Catanante, G., Istamboulie, & G., Marty, J.L. (2015). Sensitive quantitation
405 of Ochratoxin A in cocoa beans using differential pulse voltammetry based aptasensor. *Food*
406 *Chemistry, 192*, 799.804.
407
408 Muchindu, M., Iwuoha, E., Pool, E., West, N., Jahed, N. et al. (2010) Electrochemical Ochratoxin A
409 Immunosensor System Developed on Sulfonated Polyaniline. *Electroanalysis, 23*, 122-128.
410
411 Prabhakar, N., Matharu, Z., & Malhotra, B.D. (2010). Polyaniline Langmuir–Blodgett film based
412 aptasensor for ochratoxin A detection. *Biosensors and Bioelectronics, 26*, 4006–4011.
413
414 Prieto-Simon, B., Campas, M., Marty, J.L., & Noguer, T. (2008). Novel highly-performing
415 immunosensor-based strategy for ochratoxin A detection in wine samples. *Biosensor and*
416 *Bioelectronics, 23*, 995-1002.
417
418 Radi, A.E., Munoz-Berbel, X., Latesc, V., & Martyc, J.L. (2009). Label-free impedimetric
419 immunosensor for sensitive detection of ochratoxin A. *Biosensors and Bioelectronics, 24*, 1888–
420 1892.
421
422 Reddy, L., & Bhoola, K. (2010). Ochratoxins-food contaminants: impact on human health. *Toxins*,
423 *vol. 2*, 771–779.
424
425 Ricci, F., Volpe, G., Micheli, L., & Palleschi, G. (2007). A review on novel developments and
426 applications of immunosensors in food analysis. *Analytica Chimica Acta, 605*, 111-129.
427
428 Rivas, L., Mayorha-Martinez, C.C., Quesada-Gonzales, D., Zamora-Galvez, A., de la Escosura-
429 Muniz, A. & Merkoci, A. (2015). Label-Free Impedimetric Aptasensor for Ochratoxin-A Detection
430 Using Iridium Oxide Nanoparticles. *Analytical Chemistry, 87*, 5167-5172
431
432 Zhengjian, L., Wang, J., Chen, G., Deng, L. (2010). Imaging recognition events between human IgG

and rat anti – human IgG by atomic force microscopy. *International Journal of Biological Macromolecules, 47*, 661-667

List of Figures and Tables

462
463
464
465
466
467
468 Table 1
469

Schematic Biosensors Assembly	Linear Range [ng/mL]	LOD [ng/mL]	Sensitivity KΩ ml/ng	References
SPCE/4-CP/OTA-Apt	2-10	2.00	1.12	[Mishra et al., 2015]
SPCE/PTH/IrO_2NPs-OTA-Apt	$4x10^3$-$4x10^7$	$5.6 x10^3$	$2.48 x10^6$	[Rivas et al., 2015]
Au/4-CP/ Ab	2 -10	2.00	10.12	[Radi et al., 2009]
Pt/PANI-PV-SO^{3-}/Ab	$1 x10^{-2}$- $5x10^0$	$1 x10^{-2}$	0.56	[Muchindu et al., 2010]
Au /MBA/AntiOTA	$5 x10^{-3}$ -$5x10^{-2}$	$5 x10^{-3}$	20.33	This work
Au /MBA/protA-G/AntiOTA	$1 x10^{-2}$- 5	$1 x10^{-2}$	26.45	This work

470
471 SPCE screen printed carbon electrode; PTH Polythionine; Apt Aptamer; PANI-PV-SO^{3-}: Polyaniline – polyvinylsulfonate; 4-CP: 4 -
472 Carboxyphenyl ; MPA: 4 Mercaptobenzoic acid
473
474
475
476
477
478
479
480

Table 2

	Immunosensor		ELISA	
Spiked concentration [µg/kg]	**Founded concentration [µg/kg]**	**Recovery [%]**	**Founded concentration [µg/kg]**	**Recovery [%]**
1	1.04□0.04a	104.00± 5.03	1.13□0.05a	113.50 ± 4.95
1.5	1.44□0.05a	96.00□0.03	1.57□0.05a	104.69□7.00
2.5	2.41□0.03a	96.40± 4.51	2.69□0.09b	107.60 ± 5.66
5	5.46□0.30a	109.30 ± 6.10	5.13±0.12b	102.68±2.4

Values are the means of three replicates. The OTA results obtained by Immunosensors and Elisa were subjected to one-way analysis of variance. Mean values within rows followed by different letters (a,b) are significantly different (P≤ 0.05) by Student–Newman–Keuls multiple comparison test.

figure 1

Click here to download high resolution image

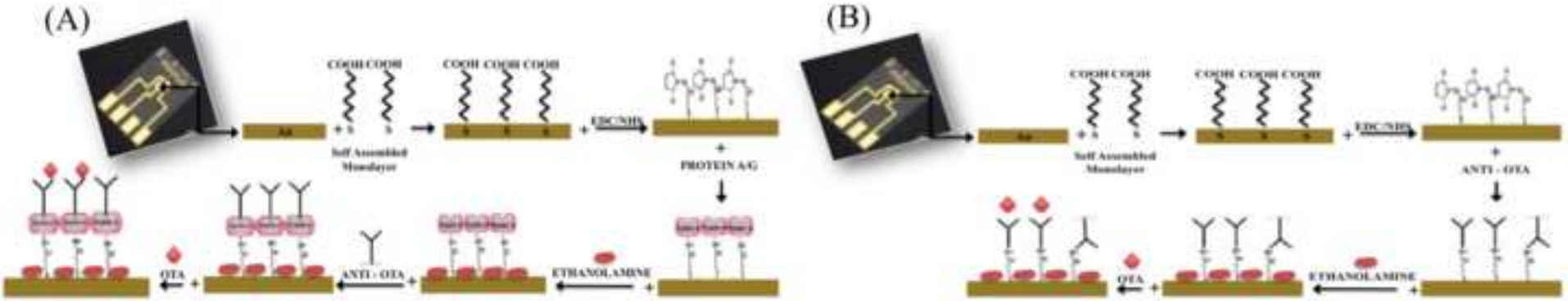

figure 2
Click here to download high resolution image

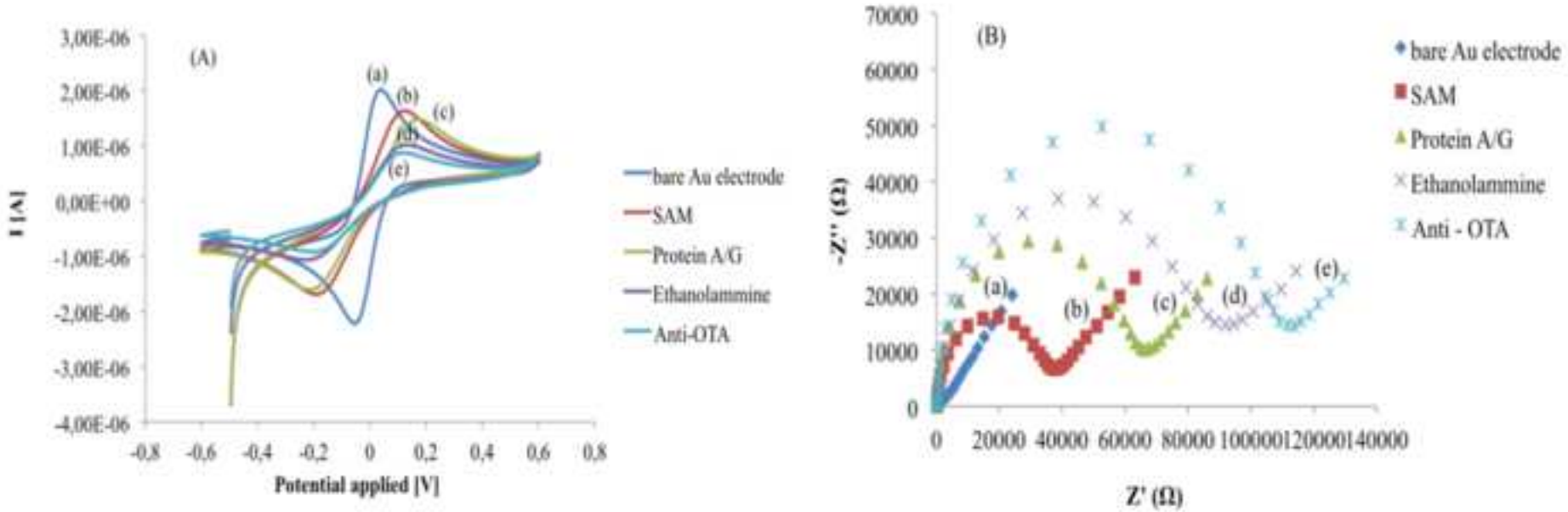

figure 3

Click here to download high resolution image

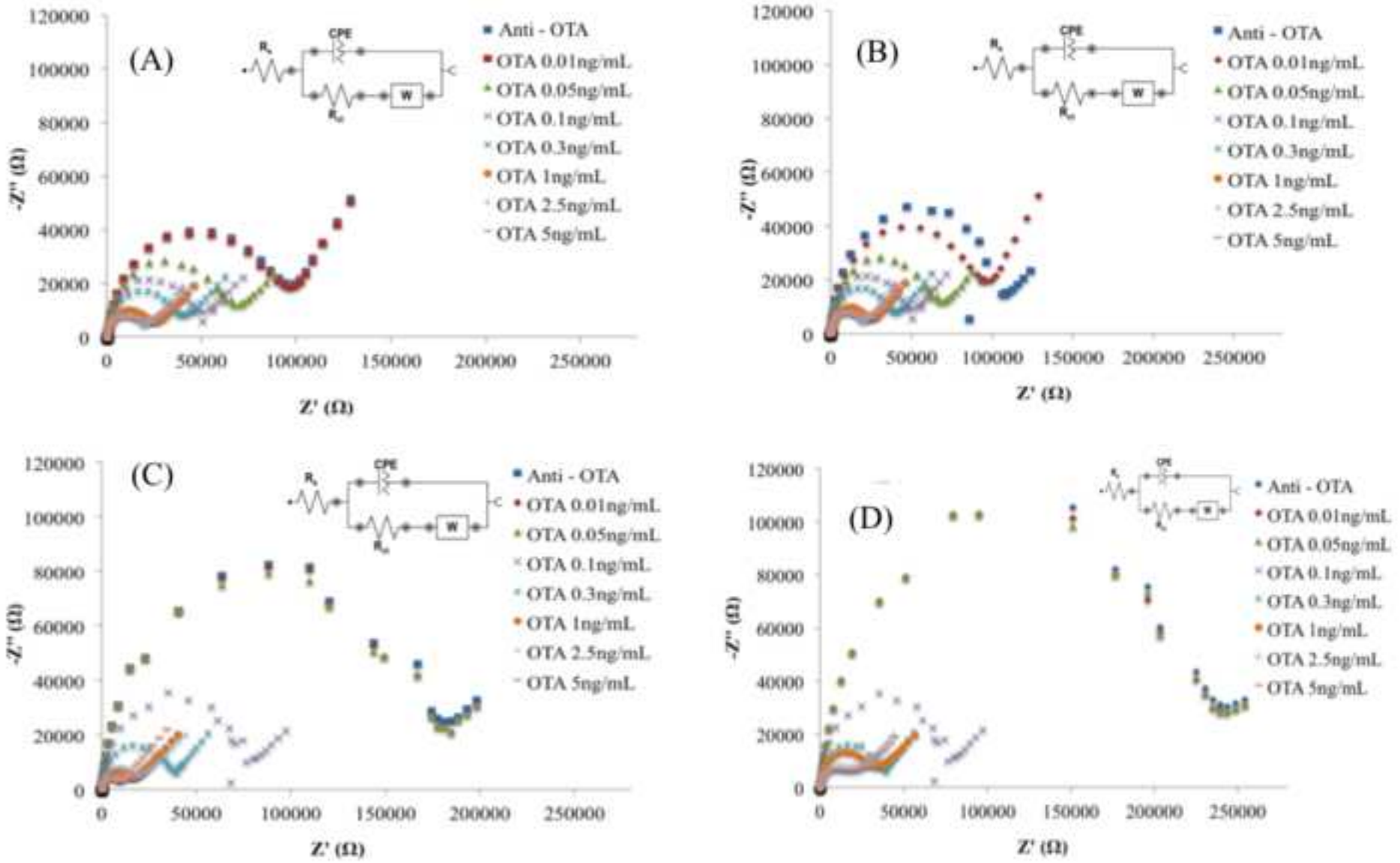

figure 4
Click here to download high resolution image